Nucleon-deuteron scattering with Δ-isobar excitation: Chebyshev expansion of two-baryon transition matrix

A. Deltuva,* K. Chmielewski, and P. U. Sauer

Institut für Theoretische Physik, Universität Hannover, D-30167 Hannover, Germany

A new technique for solving three-nucleon scattering equations is developed. It is based on the two-dimensional Chebyshev expansion of the two-baryon transition matrix. Its validity and its effectiveness are demonstrated. The dynamics of the examples is based on a two-baryon potential which allows for the excitation of a nucleon to a Δ isobar; the coupled-channel potential yields an effective three-nucleon force in the three-nucleon system. The purely nucleonic reference potential is the charge-dependent Bonn potential.

I. INTRODUCTION

We embarked on the description of nucleon-deuteron scattering with Δ-isobar excitation. Reference [1] developed a coupled-channel formulation within the framework of nonrelativistic quantum mechanics: Three-nucleon channels are coupled to those in which one nucleon is turned into a single Δ isobar. The Δ isobar is considered a stable baryon with spin and isospin $\frac{3}{2}$. The description applies to scattering energies well below the pion-production threshold. The virtual excitation of the Δ isobar yields an effective three-nucleon force, besides other Δ-isobar effects. First results of that coupled-channel description of nucleon-deuteron scattering are given for elastic scattering in Refs. [2,3], for breakup in Ref. [4] and for electromagnetic reactions in the three-nucleon system in Refs. [5,6]. Compared to Refs. [2–6], the underlying purely nucleonic reference potential is a modern one, the charge-dependent CD-Bonn potential [7].

Till now, we have solved the three-particle scattering equations in momentum space by a separable expansion of the two-baryon transition matrix. Though the validity of the separable expansion is tested in Ref. [1] and confirmed there to be quite reliable, this paper radically improves the numerical technique. Instead of using separable expansions as dynamic input, the two-baryon transition matrix is calculated exactly, but for further applications its momentum dependence is represented and effectively interpolated with the help of Chebyshev polynomials. The three-particle scattering equations are then solved without any further approximation. This interpolation scheme works for the three-particle scattering equations more efficiently than the spline interpolation.

Section II develops the Chebyshev interpolation scheme of the two-baryon transition matrix; it also describes the technique for solving the three-particle scattering equations and demonstrates its advantages. Section III tests the novel technique and gives examples of physics results for three-nucleon scattering obtained with it. Section IV presents our summary.

---

*Electronic address: deltuva@itp.uni-hannover.de; on leave from Institute of Theoretical Physics and Astronomy, Vilnius University, Vilnius 2600, Lithuania.

II. GENERAL FORMALISM

Our description of nucleon-deuteron scattering is based on the Alt-Grassberger-Sandhas (AGS) version [8] of nonrelativistic three-particle scattering theory. The symmetrized multichannel transition matrix between two-body channels $U(Z)$ and the symmetrized breakup transition matrix $U_0(Z)$ are given in Ref. [1], i.e.,

$$U(Z) = PG_0^{-1}(Z) + PT_\alpha(Z)G_0(Z)U(Z), \tag{1a}$$

$$U_0(Z) = (1+P)G_0^{-1}(Z) + (1+P)T_\alpha(Z)G_0(Z)U(Z). \tag{1b}$$

The two-baryon transition matrix $T_\alpha(Z)$ carries the dynamics; the label α indicates the interacting pair $(\beta\gamma)$ according to Fig. 1. In Eqs. (1) $G_0(Z)$ is the free resolvent $(Z-H_0)^{-1}$, H_0 being the free Hamiltonian with the inclusion of rest masses, and $P = P_{123} + P_{132}$ the sum of the cyclic and anticyclic permutation operators of three particles; Z is a general complex number and will for physical amplitudes become the available energy E for three-particle scattering, i.e., $Z = E + i0$. The term $(1+P)G_0^{-1}(Z)$ in the breakup transition matrix $U_0(Z)$ does not contribute to on-shell matrix elements of $U_0(Z)$ needed for breakup observables.

The dynamics of the description allows the interacting nucleons to be excited to a Δ isobar. A three-baryon Hilbert space is employed which has a purely nucleonic sector and a
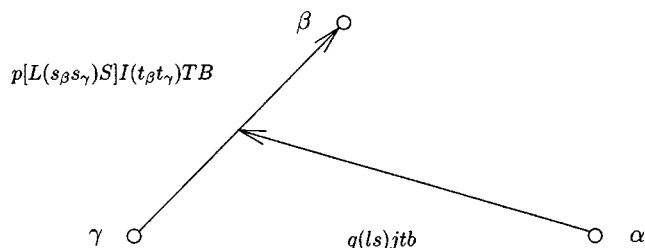
FIG. 1. Three-baryon Jacobi momenta and discrete quantum numbers. The spectator baryon is labeled α, the pair is made up of baryons β and γ. The Jacobi momenta are denoted by p and q. The abbreviation $\nu(Ij)$ for the employed partial-wave basis states $|pq\nu(Ij)\rangle_\alpha$ stands for the set $[([L(s_\beta s_\gamma)S]I(ls)j)\mathcal{J}\mathcal{M}_J[(t_\beta t_\gamma)Tt]\mathcal{T}\mathcal{M}_T Bb]$ of discrete quantum numbers.

sector in which one nucleon is replaced by a Δ isobar. The dynamics is based on a two-baryon potential which couples both sectors of the Hilbert space. The employed method for extending a purely nucleonic reference potential to a coupled-channel one is given in Ref. [9]. The notation is also taken over from Ref. [1]. The three-particle partial-wave basis states $|pq\nu(Ij)\rangle_\alpha$ of both sectors of Hilbert space, defined there as eigenstates of H_0, are used; their quantum numbers are illustrated in Fig. 1. In the following, all operators acting in the assumed Hilbert space have discrete quantum numbers. Among them, three-particle parity Π, total angular momentum $\mathcal{J}$ with projection $\mathcal{M}_\mathcal{J}$, and, if charge independence of the interaction is assumed, total isospin $\mathcal{T}$ with projection $\mathcal{M}_\mathcal{T}$, are conserved and can be fixed for the operators once and for all; due to rotational symmetry all operators are even independent of $\mathcal{M}_\mathcal{J}$, in case of charge independence even independent of $\mathcal{M}_\mathcal{T}$; we will therefore often omit those quantum numbers ($\Pi\mathcal{J}\mathcal{M}_\mathcal{J}\mathcal{T}\mathcal{M}_\mathcal{T}$) in our explicit notation. The two-baryon transition matrix in three-baryon space $T_\alpha(Z)$ which carries the dynamics is—due to geometric reasons—diagonal with respect to all discrete *spectator* quantum numbers, i.e., orbital angular momentum l, spin s, total angular momentum j, isospin t, and baryon character b. With respect to pair quantum numbers, $T_\alpha(Z)$ is—due to dynamic reasons—diagonal in the pair parity $\pi = (-)^L$, in the total pair angular momentum I and in the total pair isospin T, but it can couple states with different pair orbital angular momentum L, spin S, and baryonic content B. The abbreviation $\eta=(LSB)$ stands for all nonconserved quantum numbers, the abbreviation χ, i.e., $\chi=(\pi ITlsjtb)$, for all conserved ones. Thus, there are three sets of discrete three-particle quantum numbers, which our notation will distinguish, i.e., $\nu(Ij)=[\eta,\chi,(\Pi\mathcal{J}\mathcal{M}_\mathcal{J}\mathcal{T}\mathcal{M}_\mathcal{T})]$. However, in contrast to the two-baryon transition matrix $T_\alpha(Z)$ and to the free resolvent $G_0(Z)$, the permutation operator P in Eqs. (1) couples not only the quantum numbers η, but also the dynamically conserved quantum numbers χ.

If charge dependence is allowed for as in the calculations of this paper, the two-baryon transition matrix $T_\alpha(Z)$ becomes dependent on the projection M_T of the pair isospin T. Thus, its matrix elements in the three-particle basis $|pq\nu(Ij)\rangle_\alpha$ couple states of total isospin $\mathcal{T}=\frac{1}{2}$ and $\mathcal{T}=\frac{3}{2}$. In this case of charge dependence the discrete three-particle quantum numbers are therefore to be split up into different sets, i.e., $\nu(Ij)=[\eta,\chi,(\Pi\mathcal{J}\mathcal{M}_\mathcal{J}\mathcal{M}_\mathcal{T})]$, compared with charge independence. The total isospin $\mathcal{T}$ has to be included among the nonconserved quantum numbers $\eta=(LSBT)$. Otherwise, the formalism to be developed in this paper remains entirely unchanged.

In nucleon-deuteron scattering the transition matrices $U(Z)$ and $U_0(Z)$ act on the initial nucleon-deuteron channel state. The general nucleon-deuteron channel state $|\phi_\alpha(\mathbf{q})\nu_\alpha\rangle$ of energy $E=e_d+q^2/2M_\alpha$, e_d being the deuteron binding energy, $M_\alpha=\frac{2}{3}m_N$ being the reduced mass, and m_N the nucleon mass, is a product state of the form

$$|\phi_\alpha(\mathbf{q})\nu_\alpha\rangle=|dI_0M_IT_0M_{T_0}\rangle_\alpha|\mathbf{q}s_0m_st_0m_tb_0\rangle_\alpha, \quad (2a)$$

with $I_0=1$, $T_0=M_{T_0}=0$, and $s_0=t_0=b_0=\frac{1}{2}$; M_I, m_s and

m_t are projections of the quantum numbers I, s and t defined in Fig. 1. For computational convenience $|\phi_\alpha(\mathbf{q})\nu_\alpha\rangle$ is expanded into the partial-wave coupled states $|dq\chi_d\rangle_\alpha$ according to

$$|\phi_\alpha(\mathbf{q})\nu_\alpha\rangle$$

$$= \sum_{\mathcal{J}\mathcal{M}_\mathcal{J}\mathcal{T}\mathcal{M}_\mathcal{T}jm_jlm_l}|dq\{[I_0(ls_0)j]\mathcal{J}\mathcal{M}_\mathcal{J}(T_0t_0)\mathcal{T}\mathcal{M}_\mathcal{T}b_0\}\rangle_\alpha$$

$$\times\langle I_0M_Ijm_j|\mathcal{J}\mathcal{M}_\mathcal{J}\rangle\langle lm_ls_0m_s|jm_j\rangle$$

$$\times\langle T_0M_{T_0}t_0m_t|\mathcal{T}\mathcal{M}_\mathcal{T}\rangle Y^*_{lm_l}(\hat{\mathbf{q}}), \quad (2b)$$

with the abbreviation $|dq\chi_d\rangle_\alpha$ for the partial-wave projected nucleon-deuteron state, i.e.,

$$|dq\chi_d\rangle_\alpha\equiv|dq\{[I_0(ls_0)j]\mathcal{J}\mathcal{M}_\mathcal{J}(T_0t_0)\mathcal{T}\mathcal{M}_\mathcal{T}b_0\}\rangle_\alpha. \quad (2c)$$

In the notation $|dq\chi_d\rangle_\alpha$ of the coupled state the symbol χ_d stands for the set $(\pi_0I_0T_0ls_0jt_0b_0)$ of quantum numbers with $\pi_0=1$; there are two (three) distinct coupled states for each set of three-particle quantum numbers $(\Pi\mathcal{J}\mathcal{M}_\mathcal{J}\mathcal{M}_\mathcal{T})$ with $\mathcal{J}=\frac{1}{2}(\mathcal{J}\geqslant\frac{3}{2})$; those three-particle quantum numbers are notationally suppressed in $|dq\chi_d\rangle_\alpha$.

The solution of the integral equation (1a) for the multi-channel transition matrix $U(Z)$ for the initial energy $Z=E_i+i0$, $E_i=e_d+q_i^2/2M_\alpha$, acting on the initial nucleon-deuteron states $|dq_i\chi_{d_i}\rangle_\alpha$,

$$U(E_i+i0)|dq_i\chi_{d_i}\rangle_\alpha=\sum_{n=0}^\infty\left[PT_\alpha(E_i+i0)G_0(E_i+i0)\right]^n$$

$$\times PG_0^{-1}(E_i+i0)|dq_i\chi_{d_i}\rangle_\alpha, \quad (3)$$

is constructed from the Neumann series of finite order using the method of Padé approximants. The breakup transition matrix $U_0(Z)$ is then obtained by quadrature. Because of the permutation operator P, at each iteration step in Eq. (3) interpolation is required in at least two continuous variables, depending on the used representation of P. Usually, cubic spline interpolation is used. However, in this work we present an alternative interpolation technique in terms of Chebyshev polynomials. We do so for the two-baryon transition matrix $T_\alpha(Z)$ with respect to both the initial p and final p' relative momenta of the interacting pair. That novel interpolation technique will then yield a novel technique for solving the AGS equations (1).

Why Chebyshev polynomials? We follow the so-called *moral principle 1* of Ref. [10].

(i) When in doubt, use Chebyshev polynomials, unless the solution is spatially periodic, in which case an ordinary Fourier series is better.

(ii) Unless you are sure another set of basis functions is better, use Chebyshev polynomials.

(iii) Unless you are really, really sure that another set of basis functions is better, use Chebyshev polynomials.

Whereas the following section develops the interpolation scheme in terms of Chebyshev polynomials, Appendix A gives more formal reasons for its validity.

A. Chebyshev interpolation

The two-baryon transition matrix $T_\alpha(Z)$ in three-particle space is calculated using the full form of the two-baryon potential v_α, but for further applications $T_\alpha(Z)$ is rewritten in an approximate Chebyshev representation, employed later on for an efficient interpolation. $T_\alpha(Z)$ is of the general structure

$$T_\alpha(Z) = v_\alpha + v_\alpha G_0(Z) T_\alpha(Z), \tag{4a}$$

$$T_\alpha(Z) = v_\alpha + v_\alpha \frac{1}{Z - H_0 - v_\alpha} v_\alpha, \tag{4b}$$

$$T_\alpha(Z) = \sum_{\nu'\nu} \int p'^2 dp' \int q'^2 dq' \int p^2 dp \int q^2 dq$$
$$\times |p'q'\nu'(I'j')\rangle_{\alpha\alpha}\langle p'q'\nu'(I'j')|$$
$$\times T_\alpha(Z) |pq\nu(Ij)\rangle_{\alpha\alpha}\langle pq\nu(Ij)|. \tag{4c}$$

The two-baryon potential v_α acts between the pair $(\beta\gamma)$. According to Eq. (4b) the dependence of $T_\alpha(Z)$ on the final and initial pair momenta p' and p arises from the momentum dependence of the potential v_α; that dependence is represented in terms of Chebyshev polynomials as follows:

$$T_\alpha(Z) \approx \sum_{\nu'\nu} \int q^2 dq \int p'^2 dp' \int p^2 dp |p'q\nu'(I'j')\rangle_\alpha$$
$$\times \sum_{i',i=0}^{n_c-1} t_{L'}^{i'}(p') \delta_{\chi'\chi} T_{\eta'\eta}^{i'i}(\chi q, Z) t_L^i(p)_\alpha \langle pq\nu(Ij)|, \tag{5a}$$

$$T_\alpha(Z) = \sum_{\nu'\nu} \int q'^2 dq' \int q^2 dq$$
$$\times \sum_{i',i=0}^{n_c-1} |t^{i'}q'\nu'\rangle_\alpha (i'q'\nu'|\mathbf{T}_\alpha(Z)|iq\nu)_\alpha \langle t^i q\nu|, \tag{5b}$$

$$T_\alpha(Z) = |\mathbf{t}_\alpha\rangle \mathbf{T}_\alpha(Z)\langle \mathbf{t}_\alpha|. \tag{5c}$$

The representation (5a) of the two-baryon transition matrix is only approximate, since the expansion is in a finite number n_c of polynomials; in contrast, the manipulations leading from Eq. (5a) to Eqs. (5b) and (5c) are exact. The employed momentum functions

$$t_L^i(p) = \frac{p^L}{(p^2 + a_L^2)^{L/2}} T_i(x_c(p)) \tag{6}$$

are related to the Chebyshev polynomials $T_i(x) = \cos(i \arccos x)$, defined in the interval $[-1,1]$. $x_c(p)$

$= (p^2 - a^2)/(p^2 + a^2)$ is the function which maps the interval $[0,\infty)$ of the physical values of momentum p to the interval $[-1,1]$. The form of the mapping function $x_c(p)$ and the parameters a and a_L are chosen beforehand by experience. The parameters a and a_L are taken to be the same for all polynomials. Separating out factors of type $p^L/(p^2 + a_L^2)^{L/2}$ makes the remaining function, which is to be represented by Chebyshev polynomials, smoother and ensures correct asymptotic behavior of the expansion for small momenta of the interacting pair. The expansion parameters are the Chebyshev coefficients $T_{\eta'\eta}^{i'i}(\chi q, Z)$. They are independent of the pair label α. They are calculated for $(i',i) = 0, \ldots, N-1$, $N \geq n_c$ in Appendix A from the exact matrix elements of $T_\alpha(Z)$ at the pair momenta p_k' and p_k corresponding to all the N zeros of $T_N(x)$, i.e., $T_N(x_c(p_k)) = 0$. The representation (5a) is exact for all those momenta p_k' and p_k, provided n_c is chosen as $n_c = N$ for the number of Chebyshev polynomials [10]; in this case the representation (5a) is a true interpolation between the momenta p_k' and p_k. If $n_c < N$, the representation (5a) is an approximation also for the momenta p_k' and p_k; we shall usually choose $n_c < N$, but nevertheless we shall call representation (5a) an interpolation scheme.

In Eq. (5b) the states

$$|t^i q\nu\rangle_\alpha := \int p^2 dp |pq\nu(Ij)\rangle_\alpha t_L^i(p) \tag{7}$$

are introduced for compact notation. They arise, when interchanging the order of the summation on the Chebyshev label i and the corresponding integration on the momentum p; that interchange has to be done with care; however, we note that in all calculations only the components $_\alpha\langle p'q'\nu'(I'j')|t^i q\nu\rangle_\alpha$ of those states, together with well-behaved operators, will be needed. In Eq. (5c) the states $|t^i q\nu\rangle_\alpha$ are collected into the vector $|\mathbf{t}_\alpha\rangle$ whose components are to be differentiated by the Chebyshev label i, by the continuous variable q and by the discrete three-particle quantum numbers ν. In the same spirit, a matrix-element form is introduced in Eq. (5b) for the Chebyshev coefficients, i.e.,

$$(i'q'\nu'|\mathbf{T}_\alpha(Z)|iq\nu) := \frac{\delta(q'-q)}{q^2}\delta_{\chi'\chi} T_{\eta'\eta}^{i'i}(\chi q, Z). \tag{8}$$

Those matrix elements are collected into the operator $\mathbf{T}_\alpha(Z)$. Thus, Eq. (5c) is a concisely abbreviated form of the two-baryon transition matrix used for developing the integral equation to be solved in practice; then, the operator dependence on the continuous variable q and on the discrete three-particle quantum numbers ν has to be recovered.

A similar expansion can be given for the nucleon-deuteron states $|dq\chi_d\rangle_\alpha$, e.g., in the form

$$G_0^{-1}(E+i0)|dq\chi_d\rangle_\alpha = v_\alpha|dq\chi_d\rangle_\alpha, \tag{9a}$$

$$G_0^{-1}(E+i0)|dq\chi_d\rangle_\alpha$$

$$=\sum_\nu \int p^2 dp \int q'^2 dq' |pq'\nu(Ij)\rangle_\alpha$$

$$\times {}_\alpha\langle pq'\nu(Ij)|v_\alpha|dq\chi_d\rangle_\alpha, \qquad (9b)$$

with $E=e_d+q^2/2M_\alpha$. The resulting expansion corresponding to the expansion of the two-baryon transition matrix (5) is

$$G_0^{-1}(E+i0)|dq\chi_d\rangle_\alpha$$

$$\approx \sum_\nu \int p^2 dp |pq\nu(Ij)\rangle_\alpha \delta_{\chi\chi_d} \sum_{i=0}^{n_c-1} t_L^i(p) d_L^i, \qquad (10a)$$

$$G_0^{-1}(E+i0)|dq\chi_d\rangle_\alpha = \sum_\nu \sum_{i=0}^{n_c-1} |t^i q\nu\rangle_\alpha \delta_{\chi\chi_d} d_L^i, \qquad (10b)$$

$$(|dq\chi_d\rangle_\alpha) = G_0(E+i0)|t_\alpha\rangle\mathbf{d}. \qquad (10c)$$

The calculation of the Chebyshev coefficients d_L^i is also described in Appendix A. In Eq. (10c) the compact notation of Eq. (5c) is taken over; the round brackets on the left hand side indicate that all distinct coupled states $|dq\chi_d\rangle_\alpha$ are considered together; the matrix $\mathbf{d}$ abbreviates the $\delta_{\chi\chi_d} d_L^i$ for all those states.

The expansion (9) of $v_\alpha|dq\chi_d\rangle_\alpha$ represents the dependence of the potential v_α on the pair momentum in the same way as the corresponding expansion of the two-baryon transition matrix $T_\alpha(Z)$. Furthermore, $v_\alpha|dq\chi_d\rangle_\alpha {}_\alpha\langle dq\chi_d|v_\alpha$ builds up the residue of $T_\alpha(Z)$ at the deuteron pole; at that pole the singular factor is separated out analytically and the residue is expanded according to Eqs. (9) and (10), i.e., the Chebyshev coefficients of the two-baryon transition matrix (5a) at the deuteron pole are

$$T_{\eta'\eta}^{i'i}(\chi_d q, Z) = \frac{d_L^{i'} d_L^i}{Z-e_d-q^2/2M_\alpha}. \qquad (11)$$

B. Nucleon-deuteron scattering equations with Chebyshev representation of two-baryon transition matrix

For a given initial nucleon-deuteron state with on-shell momentum q_i, three-nucleon energy $E_i=e_d+3q_i^2/4m_N$, and initial quantum numbers χ_{d_i} the integral equation (1a) has to be solved for $U(Z)|dq_i\chi_{d_i}\rangle_\alpha$ with $Z=E_i+i0$, i.e.,

$$U(Z)|dq_i\chi_{d_i}\rangle_\alpha = [PG_0^{-1}(Z)+P|t_\alpha\rangle\mathbf{T}_\alpha(Z)$$

$$\times \langle t_\alpha|G_0(Z)U(Z)]|dq_i\chi_{d_i}\rangle_\alpha. \qquad (12)$$

Thus, the integral equation to be solved is an integral equation for $\langle t_\alpha|G_0(Z)U(Z)|dq_i\chi_{d_i}\rangle_\alpha$. It has the general structure

$$\langle t_\alpha|G_0(Z)U(Z)G_0(Z)|t_\alpha\rangle\mathbf{d}$$

$$= \langle t_\alpha|PG_0(Z)|t_\alpha\rangle\mathbf{d} + \langle t_\alpha|PG_0(Z)|t_\alpha\rangle\mathbf{T}_\alpha(Z)$$

$$\times \langle t_\alpha|G_0(Z)U(Z)G_0(Z)|t_\alpha\rangle\mathbf{d}. \qquad (13)$$

We note, that the structure of this integral equation is formally the same as Eq. (7) of Ref. [4]; it arises there from the separable expansion of the two-baryon transition matrix. In fact, any discretization of the two-baryon transition matrix $T_\alpha(Z)$, i.e., any interpolation scheme which assumes $T_\alpha(Z)$ to be calculated for a finite set of initial and final momenta and which then interpolates $T_\alpha(Z)$ to any desired momenta with the help of an expansion into a set of analytic functions, can formally be treated as a separable expansion. The form factors used in the context of the separable expansion of Ref. [4] were denoted $|\mathbf{g}_\alpha\rangle$ instead of $|t_\alpha\rangle$. The differences between $|\mathbf{g}_\alpha\rangle$ and $|t_\alpha\rangle$ are threefold.

(1) The $|\mathbf{g}_\alpha\rangle$ are independent from the spectator momentum and from the spectator discrete quantum numbers, the $|t_\alpha\rangle$ are not.

(2) Each of the $|\mathbf{g}_\alpha\rangle$ has components for all nonconserved discrete quantum numbers η, the propagator $T_\alpha(Z)$ of the separable expansion is independent of η. In contrast, each of the $|t_\alpha\rangle$ has only one component for one fixed η, since the corresponding propagator $T_\alpha(Z)$ depends on η and couples different η.

(3) Each of the distinct $G_0^{-1}(E_i+i0)|dq_i\chi_{d_i}\rangle_\alpha$ was a *single* element in the state $|\mathbf{g}_\alpha\rangle$; in contrast, each nucleon-deuteron state $G_0^{-1}(E_i+i0)|dq_i\chi_{d_i}\rangle_\alpha$ in the present context involves *all* Chebyshev polynomials considered for interpolation; this fact implies that the product $|t_\alpha\rangle\mathbf{d}$ should never be separated into its individual Chebyshev building blocks, in order to preserve a minimal number of initial states for which the integral equation (13) has to be solved.

We now explain our techniques for practically solving the integral equation (13); we make all integrations and summations, hidden in the compact form (13), explicit, i.e.,

$${}_\alpha\langle t^{i'} q'\nu'|G_0(E_i+i0)U(E_i+i0)|dq_i\chi_{d_i}\rangle_\alpha$$

$$= {}_\alpha\langle t^{i'} q'\nu'|P|dq_i\chi_{d_i}\rangle_\alpha + \sum_{i\nu}\sum_{i''\nu''}\int_0^\infty q^2 dq$$

$$\times \int_{-1}^1 dx \frac{t_L^{i'}(\bar{p}'(q',q,x))}{\bar{p}'^{L'}(q',q,x)}$$

$$\times \frac{G_{\nu'\nu}(q',q,x)}{E_i+i0-\delta\mathcal{M}-\dfrac{q'^2}{2\mu_\alpha}-\dfrac{q^2}{2\mu'_\alpha}-\dfrac{q'q}{m_\alpha}x}$$

$$\times \frac{t_L^i(\bar{p}(q',q,x))}{\bar{p}^L(q',q,x)}\delta_{\chi\chi''}T_{\eta\eta''}^{ii''}(\chi q, E_i+i0)$$

$$\times {}_\alpha\langle t^{i''} q\nu''|G_0(E_i+i0)U(E_i+i0)|dq_i\chi_{d_i}\rangle_\alpha. \qquad (14)$$

This representation of the integral equation is derived from the form

$$_\alpha\langle p'q'\nu'(I'j')|P|pq\nu(Ij)\rangle_\alpha$$

$$= \int_{-1}^{+1} dx \frac{\delta(p'-\bar{p}'(q',q,x))}{p'^{L'+2}} \frac{\delta(p-\bar{p}(q',q,x))}{p^{L+2}}$$

$$\times G_{\nu'\nu}(q',q,x) \tag{15}$$

of the permutation operator P, defined in Appendix A of Ref. [2]; the functions $\bar{p}(q',q,x)$, $\bar{p}'(q',q,x)$, and $G_{\nu'\nu}(q',q,x)$ are given there. The driving term $_\alpha\langle t^{i'}q'\nu'|P|dq_i\chi_{d_i}\rangle_\alpha$ in the integral equation (14) has to be calculated using Eq. (15); we keep it in its compact form $_\alpha\langle t^{i'}q'\nu'|P|dq_i\chi_{d_i}\rangle_\alpha$, since that part of the integral equation will not be essential for our further considerations. In Eq. (14), m_α is the mass of the spectator, $\mu_\alpha = m_\beta m_\gamma/(m_\beta+m_\gamma)$ the reduced mass of the pair, and $\delta\mathcal{M}$ the rest mass of the three-baryon state, normalized to zero for three-nucleons; since the permutation operator P only couples states with the same three-baryon content, $\delta\mathcal{M}$ is the same for the quantum numbers ν' and ν.

The kernel of the integral equation (14) contains singularities. The term $[E_i+i0-\delta\mathcal{M}-q'^2/2\mu_\alpha-q^2/2\mu'_\alpha-(q'q/m_\alpha)x]^{-1}$, arising from the free resolvent $G_0(E_i+i0)$, develops so-called *moving* singularities of kinematical origin above breakup threshold, whereas the matrix of the Chebyshev coefficients $T^{ii''}_{\eta\eta''}(\chi q,E_i+i0)$ shows the deuteron bound state pole (11). That deuteron pole is handled easily by regularization through subtraction. The treatment of the *moving* singularities is taken over from Ref. [4]; it is based on real-axis integration; changes compared with Ref. [4] required by the special form (14) of the integral equation are minimal.

The calculation of the first terms of the Neumann series (3) for $_\alpha\langle t^{i'}q'\nu'|G_0(E_i+i0)U(E_i+i0)|dq_i\chi_{d_i}\rangle_\alpha$ of Eq. (14) requires many matrix multiplications. We have two options for this step.

The *first option* follows the strategy of Refs. [2,4] for a separable expansion of the two-baryon transition matrix. When solving the integral equation (14) as in Ref. [4], the matrix elements

$$_\alpha\langle t^{i'}q'\nu'|PG_0(E_i+i0)|t^iq\nu\rangle_\alpha$$

$$= \int_{-1}^{1} dx \frac{t_{L'}^{i'}(\bar{p}'(q',q,x))}{\bar{p}'^{L'}(q',q,x)}$$

$$\times \frac{G_{\nu'\nu}(q',q,x)}{E_i+i0-\delta\mathcal{M}-\dfrac{q'^2}{2\mu_\alpha}-\dfrac{q^2}{2\mu'_\alpha}-\dfrac{q'q}{m_\alpha}x}$$

$$\times \frac{t_L^i(\bar{p}(q',q,x))}{\bar{p}^L(q',q,x)} \tag{16a}$$

are obtained first by carrying out the the x integration which involves only known functions. Correspondingly, the Born term of Eq. (14) could be calculated according to

$$_\alpha\langle t^{i'}q'\nu'|P|dq_i\chi_{d_i}\rangle_\alpha$$

$$= \sum_{i\nu} {}_\alpha\langle t^{i'}q'\nu'|PG_0(E_i+i0)|t^iq\nu\rangle_\alpha \delta_{\chi\chi_{d_i}}d_L^i, \tag{16b}$$

starting from $_\alpha\langle t^{i'}q'\nu'|PG_0(E_i+i0)|t^iq\nu\rangle_\alpha$. The integral equation (14) is then solved in one continuous variable, i.e., in the spectator momentum q. That procedure is a viable one, and we refer to it as the separable expansion technique for solution. However, that technique is very uneconomical in case of a substantial number of Chebyshev polynomials in the adopted interpolation scheme; that number is usually much larger than the corresponding ranks of the separable expansion in Refs. [1–4]. The matrix $_\alpha\langle t^{i'}q'\nu'|PG_0(E_i+i0)|t^iq\nu\rangle_\alpha$ is of formidable size, it typically requires computer storage of the order of 100 GB; thus, it can not be stored in any medium-sized computer and has to be computed many times when calculating the Neumann series (3). Besides that, it couples all labels and quantum numbers $(iq\nu)$ with each other yielding lengthy matrix multiplications, whereas all building blocks within the form (16a) of $_\alpha\langle t^{i'}q'\nu'|PG_0(E_i+i0)|t^iq\nu\rangle_\alpha$ have block-diagonal structure.

In the *second option* the same Neumann series (3) is calculated. However, the integrations and summations in Eq. (14) are carried out, whenever they arise, starting from right to left. This is the natural order of matrix multiplications taking advantage of the block-diagonal structure of the quantities entering Eq. (14). This procedure reduces the number of required floating point operations considerably. The Born term $_\alpha\langle t^{i'}q'\nu'|P|dq_i\chi_{d_i}\rangle_\alpha$ is calculated also directly without any reference to the matrix elements (16a). That important logistic change constitutes the new technique of this paper for solving the AGS equations, compared with the technique of separable expansion, called *first option* in this paper and used by us before in Refs. [1–4].

Finally, the partial-wave projected matrix elements needed for the calculation of the observables of elastic and inelastic nucleon-deuteron scattering follow from $_\alpha\langle t^{i'}q\nu'|G_0(E_i+i0)U(E_i+i0)|dq_i\chi_{d_i}\rangle_\alpha$ in the forms

$$_\alpha\langle dq_i\chi_{d_f}|U(E_i+i0)|dq_i\chi_{d_i}\rangle_\alpha$$

$$= {}_\alpha\langle dq_i\chi_{d_f}|PG_0^{-1}(E_i+i0)|dq_i\chi_{d_i}\rangle_\alpha$$

$$+ \sum_{i\nu} \int_0^\infty q^2 dq \, {}_\alpha\langle dq_i\chi_{d_f}|P|t^iq\nu\rangle_\alpha$$

$$\times \sum_{i'\nu'} \delta_{\chi\chi'} T^{ii'}_{\eta\eta'}(\chi q,E_i+i0)$$

$$\times {}_\alpha\langle t^{i'}q\nu'|G_0(E_i+i0)U(E_i+i0)|dq_i\chi_{d_i}\rangle_\alpha, \tag{17a}$$

$$_\alpha\langle pq\nu(Ij)|T_\alpha(E_i+i0)G_0(E_i+i0)U(E_i+i0)|dq_i\chi_{d_i}\rangle_\alpha$$

$$=\sum_i t_L^i(p)\sum_{i'\nu'}\delta_{\chi\chi'}T_{\eta\eta'}^{ii'}(\chi q,E_i+i0)$$

$$\times{}_\alpha\langle t^{i'}q\nu'|G_0(E_i+i0)U(E_i+i0)|dq_i\chi_{d_i}\rangle_\alpha. \quad (17b)$$

Equations (17) suggest that it is more convenient to solve Eq. (14) for $\sum_{i'\nu'}\delta_{\chi\chi'}T_{\eta\eta'}^{ii'}(\chi q,E_i+i0)_\alpha\langle t^{i'}q\nu'|G_0(E_i+i0)U(E_i+i0)|dq_i\chi_{d_i}\rangle_\alpha$ instead for $_\alpha\langle t^{i'}q\nu'|G_0(E_i+i0)U(E_i+i0)|dq_i\chi_{d_i}\rangle_\alpha$. The former quantity is directly needed in Eqs. (17); it corresponds to the alternative form $\mathcal{T}(Z)=T_\alpha(Z)G_0(Z)U(Z)$ of the multichannel transition matrix used in Ref. [11]. The on-shell elements of the symmetrized multichannel transition matrix $U(E_i+i0)$ between two-body channels (2a) are obtained from the result (17a). The on-shell elements of the symmetrized breakup transition matrix $U_0(E_i+i0)$ are obtained from the result (17b) according to Eq. (1b); it is advantageous to transform the matrix elements (17b) first to plane-wave basis and then to apply also the permutation operator P of the part $(1+P)$ according to Eq. (1b) in that plane-wave basis.

III. RESULTS

First, this section tests the efficiency of the Chebyshev expansion for the two-baryon transition matrix and for the deuteron wave function. Second, the Chebyshev expansion is employed as an interpolation scheme when solving the three-particle scattering equations with the two-baryon transition matrix as dynamic input. In this context, our numerical scheme is tested for accuracy and the advantage of the use of the Chebyshev expansion is discussed. Furthermore, we give new physics results for elastic nucleon-deuteron scattering and nucleon-deuteron breakup.

Unless otherwise stated, our calculations are based on the purely nucleonic CD-Bonn potential [7]; it is extended as the Paris potential in Ref. [9] to include the Δ isobar degree of freedom. The CD-Bonn potential allows for charge dependence in the isospin triplet partial waves up to $I=4$. The coupled-channel potential derived from CD-Bonn shows the same charge dependence. The charge dependence of the nucleon-nucleon interaction is treated exactly in the $^1S_0$ partial wave, yielding total isospin $\mathcal{T}=\frac{3}{2}$ channels; in other two-baryon isospin triplet partial waves up to $I=4$ the charge dependence is treated approximately, i.e., without coupling to $\mathcal{T}=\frac{3}{2}$ states; this approximate treatment weights the components of the isospin triplet partial waves in the ratio $\frac{1}{3}:\frac{2}{3}$ for the proton-neutron and neutron-neutron parts; in those higher partial waves the coupling to $\mathcal{T}=\frac{3}{2}$ states was checked to be quantitatively irrelevant.

Partial waves up to total two-baryon angular momentum $I=5$ in purely nucleonic channels and up to $I=4$ in nucleon-Δ channels and up to total three-baryon angular momentum $\mathcal{J}=\frac{27}{2}$ are taken into account. The results appear fully converged with respect to higher two-baryon angular momenta I, with respect to higher three-baryon angular momenta $\mathcal{J}$, and with respect to Δ-isobar coupling on the scale of accuracy which present-day experimental data require.

The calculations are in momentum space and leave the Coulomb interaction between the charged particles out. Though most data taken for the comparison with theoretical predictions are from proton-deuteron scattering, the calculations therefore refer to the neutron-deuteron system; correspondingly, the calculations of the trinucleon bound state in Appendix B refer to tritium. We use the neutron-neutron and proton-neutron components of the CD-Bonn and the coupled-channel two-baryon potentials. In the free Hamiltonian H_0, we use an averaged nucleonic mass $m_N = 938.919$ MeV, in order to ensure charge independence for the moving singularities in the integral equation (14). Due to this choice of masses the neutron-neutron transition matrix is calculated differently compared with Ref. [7], which carried out the fit to data; the resulting difference in neutron-neutron phase shifts between this paper and Ref. [7] is entirely negligible. The mass of the Δ isobar is assumed to be 1232 MeV.

A. Test of Chebyshev expansion of the two-baryon transition matrix and of the deuteron wave function

The Chebyshev expansion works equally well for the two-baryon transition matrix according to Eq. (5) and for the deuteron wave function according to Eqs. (10). Figure 2 displays examples of the Chebyshev coefficients $T_{\eta'\eta}^{i'i}(\chi q,Z)$ of the two-baryon transition matrix and of the Chebyshev coefficients d_L^i of $v_\alpha|dq\chi_d\rangle_\alpha$; their fast decrease with increasing order of the polynomial is impressive; the convergence appears subgeometric as described in Appendix A; the expansion converges therefore rapidly as shown in Fig. 3. Thus, the truncation of the Chebyshev expansion at the rather small orders 16 or 24 is well justified, except for very large momenta, unimportant for three-nucleon scattering at the rather modest available energies considered in this paper. The Chebyshev expansion is systematic and efficient; in contrast, when using spline interpolation for the same quantities all spline functions are of same importance; there is no way for a corresponding systematic truncation of the spline expansion.

B. Test of new technique for solving integral equation (14) using Chebyshev expansion

We performed the following tests, in order to assure the technical reliability of our numerical apparatus, called *second option* in Sec. II B.

(1) References [1–4] employed the coupled-channel potential A2 [9] and the Paris potential [12] as its nucleonic reference potential in separable forms as dynamic input for calculations. We take those separable forms now as numerical test cases, but do not exploit their separable structure. Instead, we use a Chebyshev expansion for their separable expansions and interpolate them accordingly when solving integral equation (14) with the technique of the *second option* of Sec. II B. The agreement with all previous results of Refs. [2,4] is so excellent that differences cannot be documented in any plot. This fact is one indication that the new technique for solving the integral equation (14) is reliable.
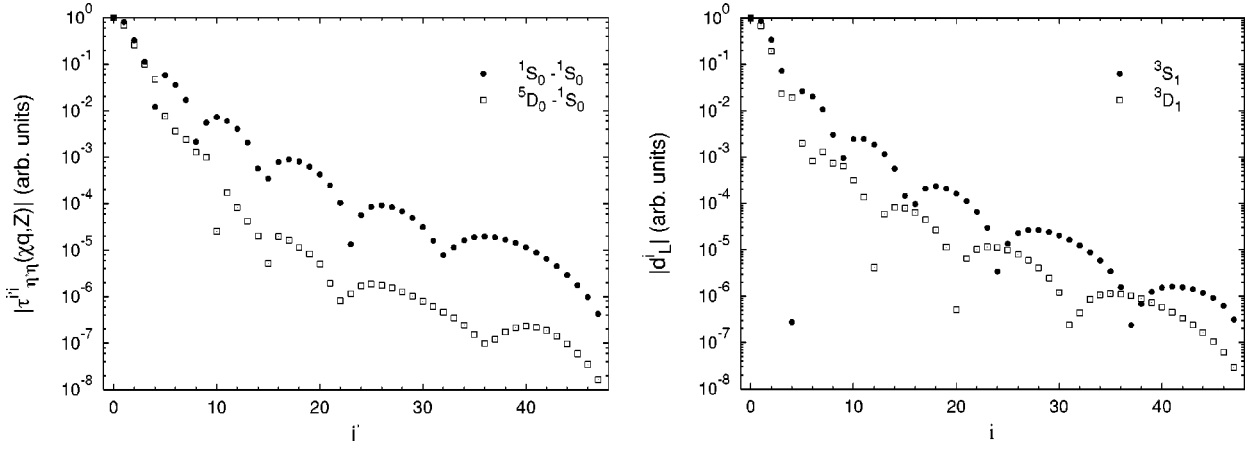
FIG. 2. Chebyshev coefficients $T^{i'i}_{\eta'\eta}(\chi q,Z)$ of the $^1S_0(NN)-^5D_0(N\Delta)$ two-baryon transition matrix for $i=1$, $q=0$, and $Z=100$ MeV and Chebyshev coefficients d^i_L of the deuteron wave function as functions of the order i' or i of the Chebyshev polynomials.

(2) In Sec. II B two options for solving the basic integral equation (14) with Chebyshev interpolation of the two-baryon transition matrix and the deuteron wave function are discussed; the technique preferred by us is the *second option*. Since both techniques differ only in the order of matrix multiplications, they have to yield identical results. In fact, they do so in our test calculations within at least ten significant figures and thereby prove the numerical reliability of that part of our calculational scheme. These test calculations also prove our expectation, that the technique of the *second option* is the much more economical one for solving the integral equation (14), being faster by a factor of the order of 10 than the separable expansion of the *first option* technique. Furthermore, the actual computer time for the technique of the *second option* depends only weakly on the number of Chebyshev polynomials employed, whereas in the case of the technique of the *first option* it increases quadratically

with that number; the ratio is about 10 when using 24 Chebyshev polynomials.

(3) Figure 4 studies the convergence of sample physics observables with the number of Chebyshev polynomials employed. The convergence is impressively rapid. Understandably it is faster for lower energies. The Chebyshev expansion is favored by us and will be used by us from now on. Nevertheless, as an alternative, also spline interpolation is used, as usually adopted in few-body numerics when solving the integral equation (14). In both interpolation schemes the integral equation (14) has the same general structure as discussed in Appendix C. The results provided by both interpolation schemes are indistinguishable; however, spline interpolation reaches the same quality of results only with a considerably larger number of functions than the corresponding Chebyshev expansion. The results of Fig. 4 confirm our previous conclusion: *The Chebyshev expansion is systematic*
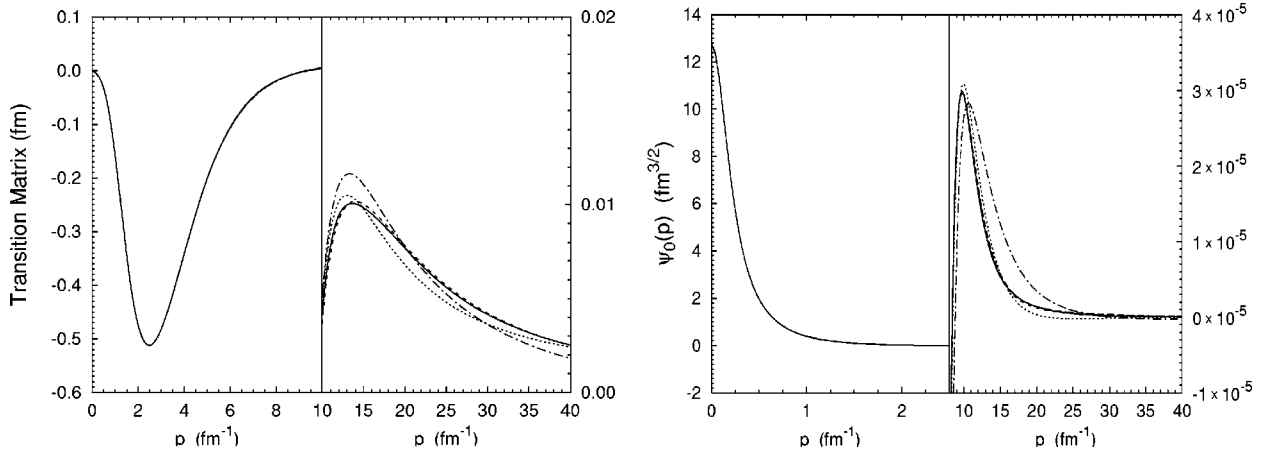
FIG. 3. Convergence of the Chebyshev expansion. On the left side the real part of the $^1S_0(NN)-^5D_0(N\Delta)$ two-baryon transition matrix is shown as function of the final momentum p. The transition $^1S_0\rightarrow^5D_0$ at $q=0$ with the available energy $Z=100$ MeV for the initial pair momentum $p_i=1$ fm^{-1} is plotted. On the right side the $L=0$ component of the deuteron wave function $\psi_L(p) \equiv \langle p(LS)I_0M_IT_0M_{T_0}B|dI_0M_IT_0M_{T_0}\rangle$ is shown. The dot-dashed, dotted, dashed, and solid curves correspond to Chebyshev interpolation using 12, 16, 24, and 48 polynomials, respectively. All curves are indistinguishable in the resolution adopted for momenta up to 10 fm^{-1}. Differences can only be seen for momenta beyond 10 fm^{-1} with an especially fine resolution. The standard of reference is spline interpolation with 48 spline functions. The solid curves turn out to be identical with those reference curves.
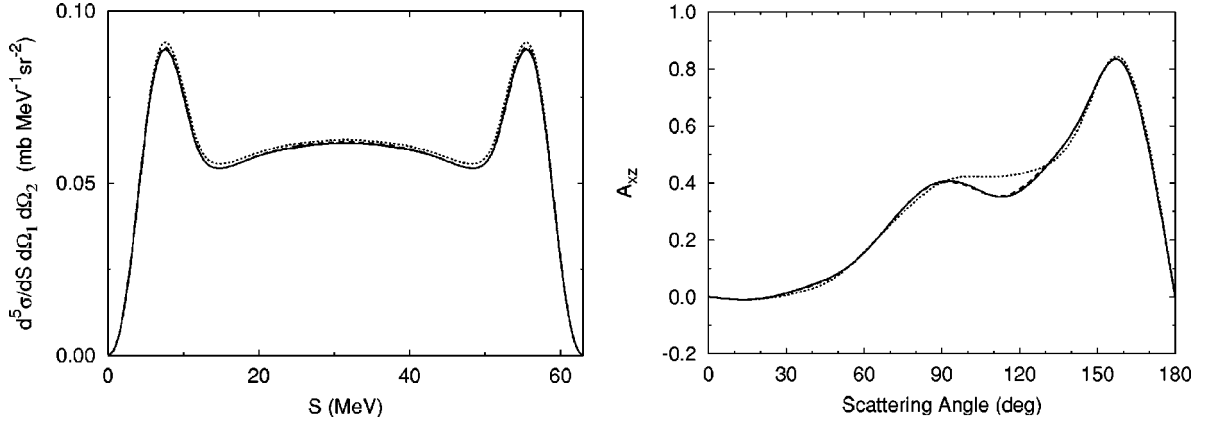
FIG. 4. Fivefold differential cross section for nucleon-deuteron breakup at 65 MeV nucleon lab energy in the space star configuration $(54.0°,54.0°,120.0°)$ and deuteron analyzing power A_{xz} for elastic nucleon-deuteron scattering at 135 MeV nucleon lab energy. The convergence of the Chebyshev expansion is studied. The dotted and dashed curves are results obtained with eight and 12 Chebyshev polynomials, respectively, the solid curve corresponds to the indistinguishable results obtained with 16, 24, and 48 Chebyshev polynomials and with 48 spline functions; always more than 24 spline functions are needed to reproduce the solid curve very well.

and efficient and thereby superior to spline interpolation. All results which are given in Secs. III C and III D are obtained with 24 Chebyshev polynomials.

C. Test of separable expansion

The quality of the separable expansion employed in Refs. [1–4] is well established for the purely nucleonic reference potential; for the two-baryon coupled-channel potential the separable expansion could be tested in the two-nucleon system and for the three-nucleon bound state and was found to be quite accurate [1]. We are now able to complete the latter tests also for three-nucleon scattering. Sample results based on the coupled-channel potential A2 of Refs. [1–4] and obtained from the integral equation (14) are compared in Fig. 5 with corresponding results for the separably expanded form of A2 derived either from the integral equation (14) or by the technique of Ref. [4]. Differences of results obtained for the separably expanded and the unexpanded forms of A2 are

discernible, but the separable expansion is again proven to be quite reliable, enforcing the conclusions of Ref. [1].

D. New physics results

The calculations of Refs. [1–4] required separable expansions for the dynamic input of the three-nucleon scattering equations; only the two-baryon coupled-channel potentials, derived from the nucleonic Paris [1] and Bonn B [15] potentials have been available to us, and both potentials are rather outdated. Furthermore, the calculations of Refs. [1–4] used only rather low partial waves, not sufficient for full convergence at higher scattering energies. Those restrictions are now gone. We therefore use the CD-Bonn potential [7] and extend it for Δ-isobar excitation as in Ref. [9]. Sample results for a variety of physics aspects of nucleon-deuteron scattering is now given. The short-hand for specifying the kinematics to which breakup observables refer is taken over from Ref. [4].
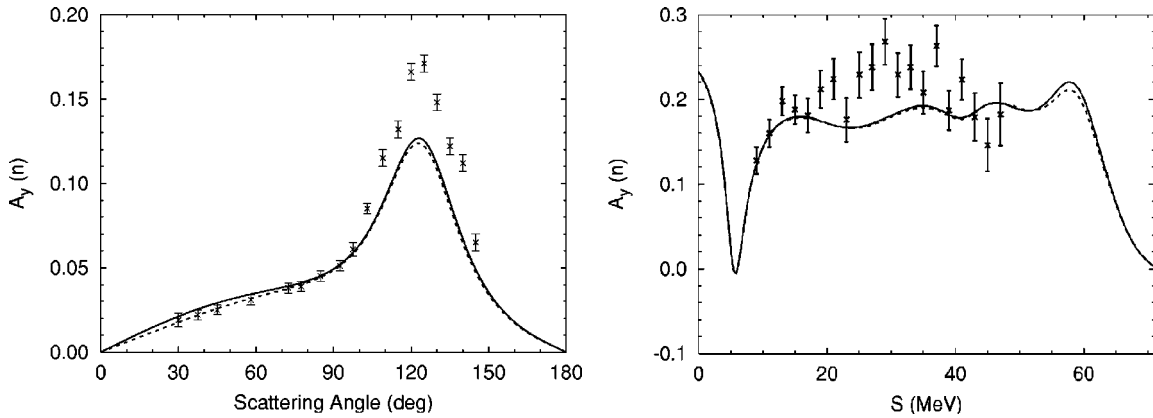
FIG. 5. Nucleon analyzing power A_y for elastic nucleon-deuteron scattering as function of c.m.scattering angle at 10 MeV nucleon lab energy and for nucleon-deuteron breakup as function of arclength S along the kinematical curve at 65 MeV nucleon lab energy in the collinear configuration $(30.0°,98.0°,180.0°)$. The separable expansion of the underlying two-baryon potential A2 with Δ-isobar excitation is tested. The dashed curves are results of the separably expanded potential form, the solid curves of the unexpanded form. The experimental data are from Refs. [13,14].
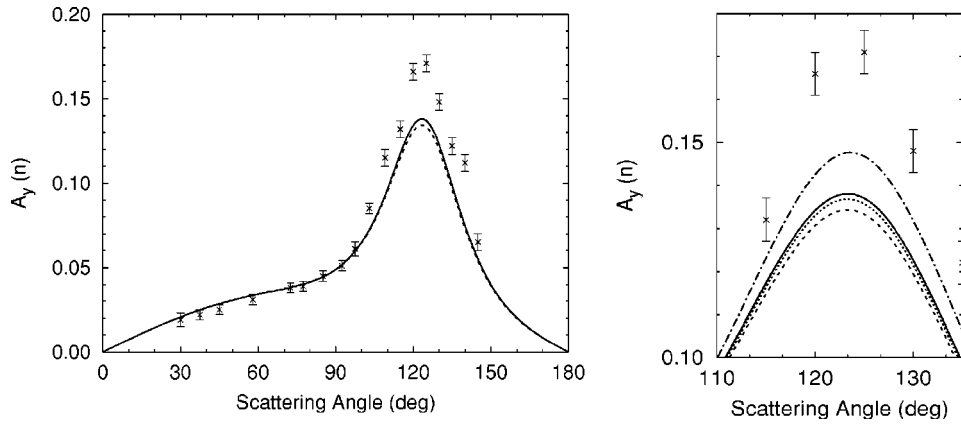
FIG. 6. Neutron analyzing power $A_y(n)$ as function of the c.m.scattering angle for elastic neutron-deuteron scattering at 10 MeV nucleon lab energy. Results of the coupled-channel potential with Δ-isobar excitation including spin-orbit interaction (solid curve) are compared with results of the CD-Bonn potential (dashed curve). On the right side the peak results are shown in finer resolution; there also the result for Δ-isobar excitation without spin-orbit interaction (dotted) is shown. The partial three-nucleon force effect arising from the Δ isobar with spin-orbit interaction is given for comparison (dashed dotted). The experimental data are from Ref. [14].

(1) Before entering the discussion of nucleon-deuteron scattering, we want to draw the attention of the reader to Appendix B. There, the hadronic properties of the tritium bound state, as derived by the technique of this paper from the CD-Bonn potential and from its coupled-channel extension to single Δ-isobar excitation, are listed. For comparison, results based on the AV18 [16] and Nijmegen [17] potentials are also given. Due to its strong nonlocality and therefore
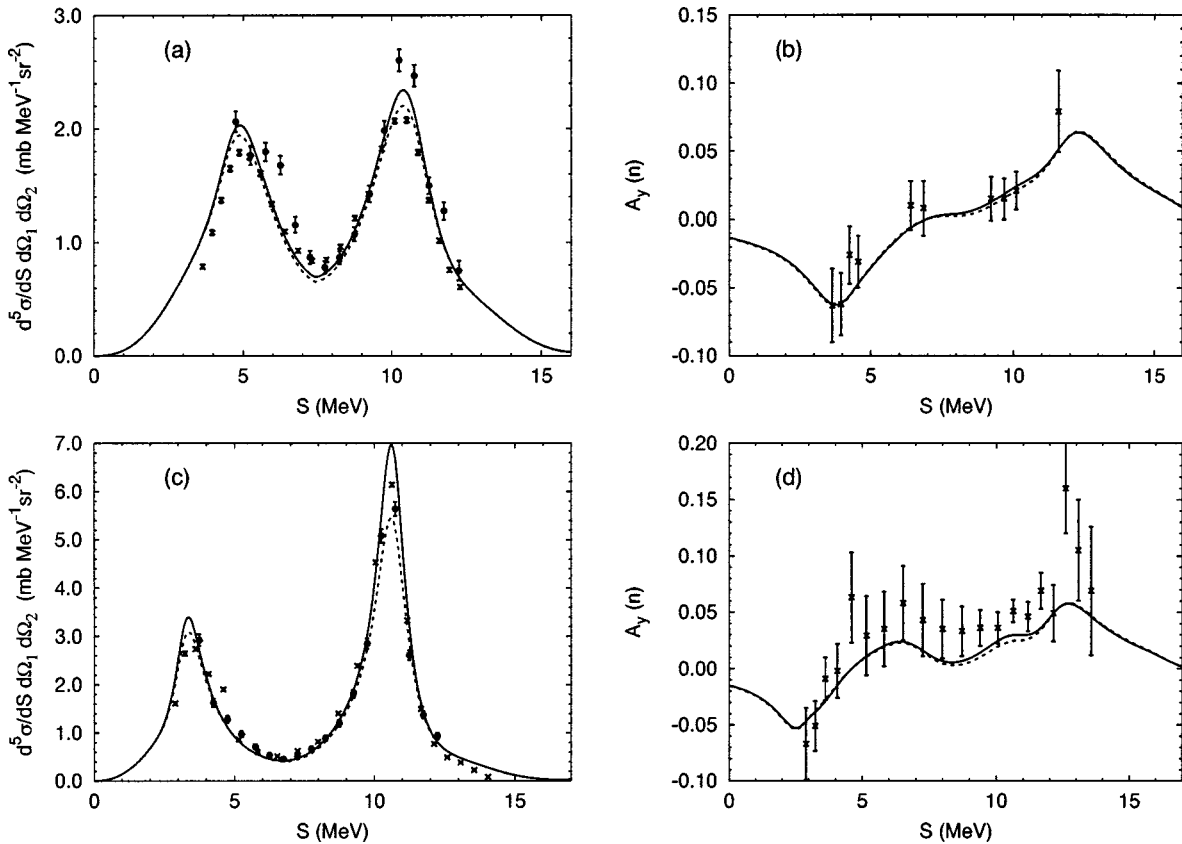
FIG. 7. Differential cross section and nucleon analyzing power $A_y(n)$ as function of the arclength S along the kinematical curve for two configurations of nucleon-deuteron breakup at 13 MeV nucleon lab energy: (a),(b) collinearity configuration (50.5°,62.5°,180.0°) and (c),(d) FSI configuration (39.0°,62.5°,180.0°). Results of the coupled-channel potential with Δ-isobar excitation are shown. The results shown as solid curves take the charge dependence in the $^1S_0$ partial wave fully into account, i.e., with coupling to three-particle channels with total isospin $\frac{3}{2}$. That coupling is left out in the results shown as dashed curves. The experimental data are from Ref. [19] referring to neutron-deuteron scattering (circles) and from Ref. [20] referring to proton-deuteron scattering (crosses).
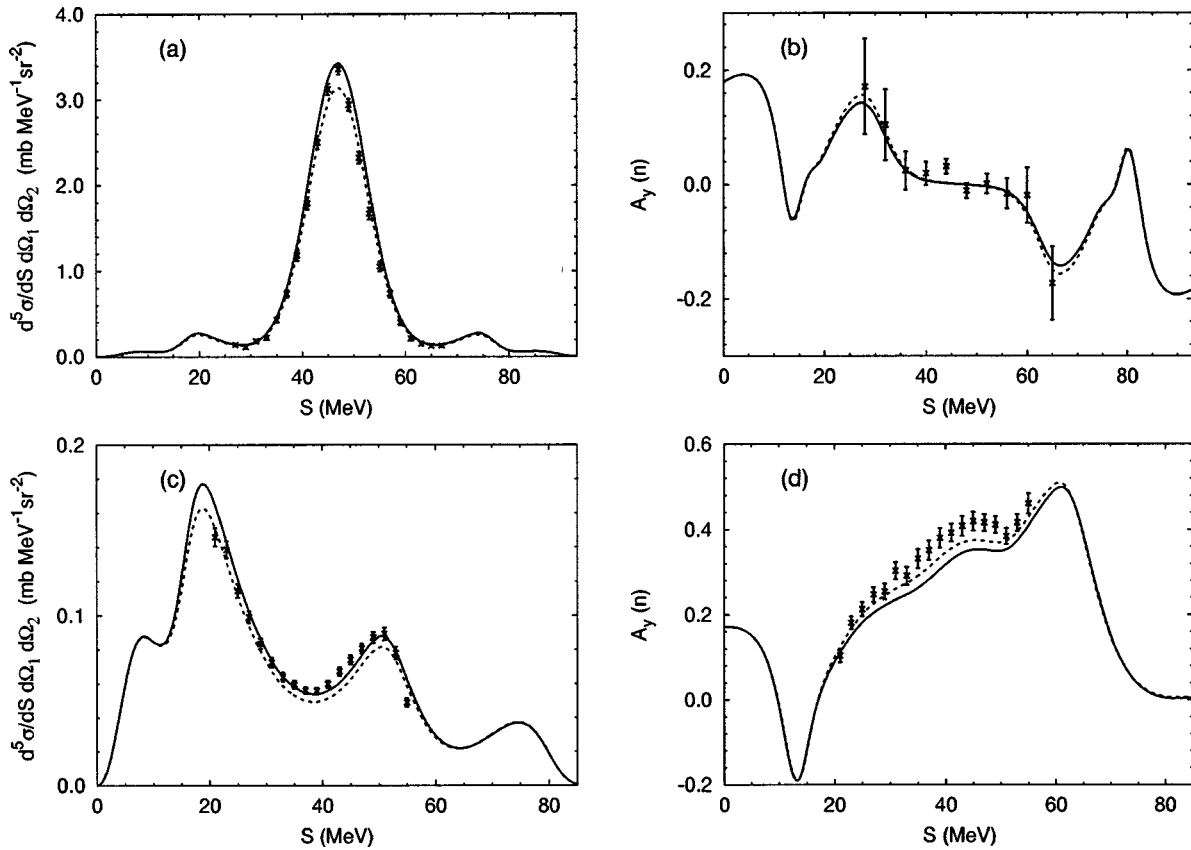
FIG. 8. Differential cross section and nucleon analyzing power $A_y(n)$ as function of the arclength S along the kinematical curve for various configurations of nucleon-deuteron breakup at 65 MeV nucleon lab energy: (a),(b) QFS configuration (44.0°,44.0°,180.0°) and (c),(d) collinear configuration (45.0°,75.6°,180.0°). Results of the coupled-channel potential with Δ-isobar excitation (solid curve) are compared with results of the CD-Bonn potential (dashed curve). The experimental data are from Refs. [13,21] and refer to proton-deuteron scattering.

due to a comparatively weak tensor force, the CD-Bonn potential provides more trinucleon binding than the local AV18, and Nijmegen II potentials or the only mildly nonlocal Nijmegen I potential. The respective coupled-channel potentials with Δ-isobar excitation show the well-known competition between two physically distinct Δ-isobar effects, i.e., the repulsive two-nucleon dispersion and the three-nucleon attraction. The coupled-channel potential derived from CD-Bonn potential still misses the tritium binding, but the remaining discrepancy is quite small.

(2) Results for the neutron analyzing power $A_y(n)$ of elastic neutron-deuteron scattering at 10 MeV nucleon lab energy are given in Fig. 6. This observable is haunted by a persistent discrepancy with theoretical predictions, called the A_y puzzle. All calculations based on realistic two-nucleon potentials and complemented by a three-nucleon force, either by an irreducible one or by an effective one as due to Δ-isobar excitation, are unable to account for the experimental height of the peak. Reference [18] discusses a three-nucleon force as possible remedy which has a phenomenological spin-orbit component with rather long range. We therefore test an effective three-nucleon force which obtains a microscopically motivated spin-orbit component arising from the spin-orbit part of the ρ-meson exchange mediating single Δ-isobar excitation; that spin-orbit component is of rather short range, its strength and range being predeter-

mined by the ρ parameters used in the standard transition potential from two-nucleon to nucleon-Δ states. The obtained results are disappointing: The inclusion of the spin-orbit mechanism of ρ exchange does not significantly decrease the long-standing discrepancy. Although the three-nucleon force effect is quite significant, it is canceled by the dispersive effect, leaving the full Δ-isobar effect small. A similar small effect is found for the deuteron vector analyzing power iT_{11}. The effect of the spin-orbit contribution to Δ-isobar effects is negligible for other observables.

(3) Results for spin-averaged and spin-dependent observables of nucleon-deuteron break-up at 13 MeV nucleon lab energy are given in Fig. 7. The proper treatment of charge dependence, including three-baryon partial waves with total isospin $\mathcal{T}=\frac{1}{2}$ and $\mathcal{T}=\frac{3}{2}$, is necessary in order to reproduce the height of the differential cross section peaks at arclength S around 10 MeV in the collinearity and in the FSI configurations of Figs. 7(a) and 7(c), the corresponding spin observables appear only mildly affected. In contrast to charge dependence, the effect of the Δ isobar is irrelevant at this scattering energy; it is therefore not separately documented in the figure.

(4) Sample results for nucleon-deuteron breakup at 65 MeV nucleon lab energy are given in Fig. 8. The effects of the Δ isobar and of its mediated three-nucleon force become more noticeable at this higher energy in some observables,
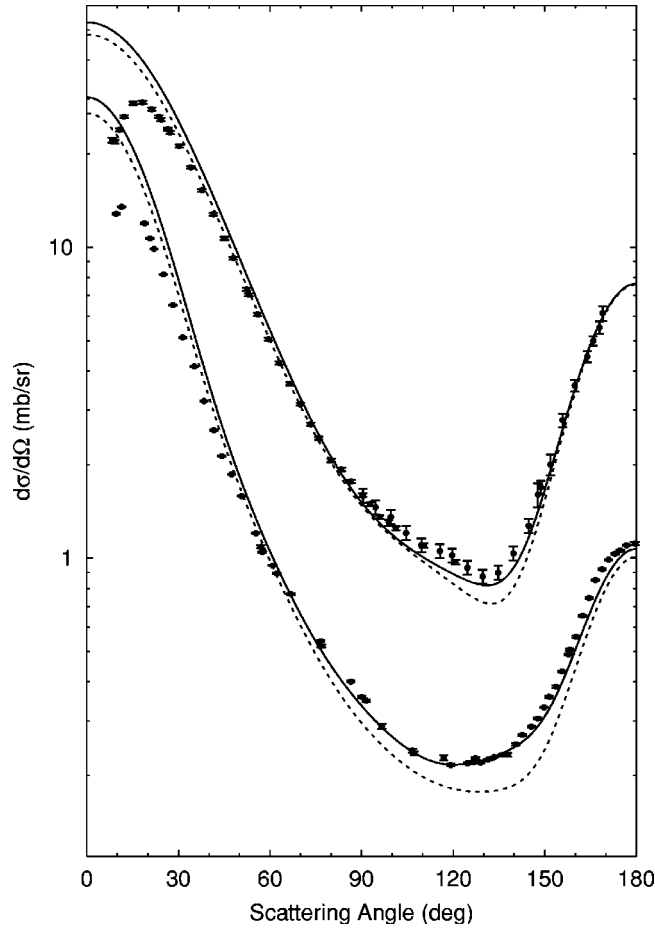
FIG. 9. Differential cross section as function of the c.m. scattering angle at 65 MeV (upper curves) and 135 MeV (lower curves) nucleon lab energy. Results of the coupled-channel potential with Δ isobar excitation (solid curves) are compared with results of the CD-Bonn potential (dashed curves). The experimental data are from Refs. [22,23] and refer to proton-deuteron scattering.

FIG. 10. Nucleon analyzing power $A_y(n)$ of elastic nucleon-deuteron scattering as function of the c.m. scattering angle at 120, 135, 150, and 170 MeV nucleon lab energy. Results of the coupled-channel potential with Δ isobar excitation (solid curves) are compared with results of the CD-Bonn potential (dashed curves). The experimental data are from Ref. [24] and refer to proton-deuteron scattering.

e.g., for the differential cross section in collinear configurations, as shown in Fig. 8(c).

(5) The Sagara discrepancy of elastic nucleon-deuteron scattering is revisited. Figure 9 shows the spin-averaged differential cross section and Fig. 10 the nucleon analyzing power at various energies. The removal of the Sagara discrepancy in the diffraction minima of the elastic differential nucleon-deuteron cross sections by the three-nucleon force derived from the Δ isobar is confirmed; the same effect is found in the minima of the nucleon analyzing power. The theoretical predictions miss the experimental data in forward direction up to an scattering angle of about 40°; this discrepancy is due to the omission of the Coulomb interaction between protons.

(6) Compared to our previous results based on the Paris potential [12] and its extension to the inclusion of a Δ isobar, most observables of elastic nucleon-deuteron scattering and of breakup get changed in predictions based on CD-Bonn and its extension. We show two typical examples in Fig. 11, where also predictions of AV18 and the Nijmegen potentials are given for comparison. The results of the modern potentials are very close to each other, but differ markedly from those of the Paris potential. The modern potentials incorporate the charge dependence of the two-nucleon interaction and are fitted to more modern data, unavailable when the Paris potential was created. Since the difference in fits is responsible for the difference in predictions, Fig. 11 only shows results with purely nucleonic reference potentials. The difference in the sample prediction for nucleon-deuteron breakup at 13 MeV nucleon lab energy reflects the charge dependence of the modern potentials which is not taken into account in the Paris potential; the difference in the sample prediction for elastic nucleon-deuteron scattering at 135 MeV nucleon lab energy reflects the improved fit of the modern potentials to more recent spin observables of two-nucleon scattering.

(7) In the discussion of items 1 to 6, we conclude that the use of well-fitted two-nucleon potentials appears important. In this respect, the CD-Bonn potential is beyond doubt a
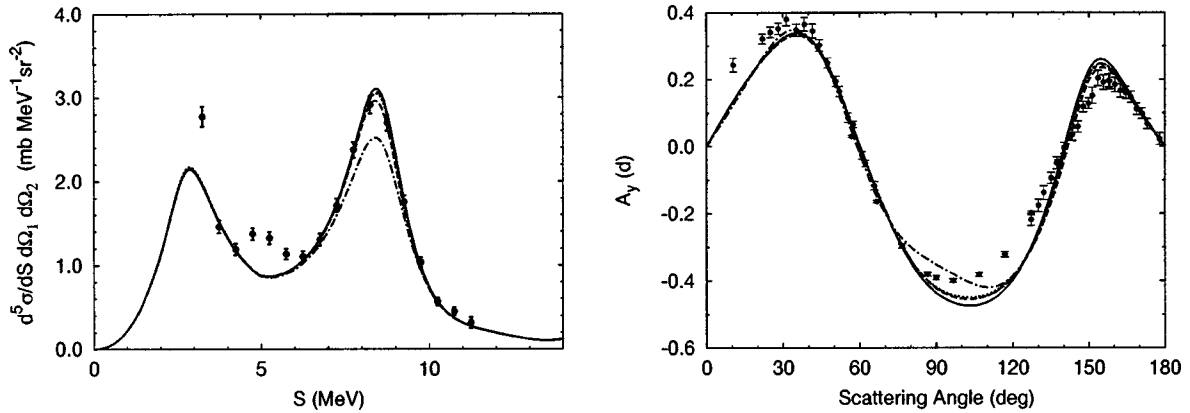
FIG. 11. Comparison of observables derived from various potentials, i.e., CD-Bonn (solid), AV18 (long-dahed), Nijmegen I (short-dashed), Nijmegen II (dotted), and Paris (dashed dotted). Differential cross section of nucleon-deuteron breakup as function of the arclength S along the kinematical curve at 13 MeV nucleon lab energy in collinear configuration (39.0°,75.5°,180.0°) and deuteron analyzing power $A_y(d)$ of elastic nucleon-deuteron scattering as function of the c.m. scattering angle at 135 MeV nucleon lab energy are shown. All predictions refer to the purely nucleonic reference potentials. The results of the modern potentials cluster around each other and are hardly distinguishable from each other in the plots. The experimental data are from Refs. [19,22].

realistic potential as the modern two-nucleon potentials [16,17] used under item (6) in this section and in Appendix B. However, we start to worry about our procedure [9] for constructing coupled-channel potentials with single Δ-isobar excitation in isospin triplet partial waves: We avoid a careful fit and only make sure that exact phase equivalence is achieved at zero kinetic energy. Thus, phase differences between the nucleonic reference potential and the coupled-channel potential arise, in general, and increase with increasing energy; e.g., at 100 MeV nucleon lab energy the phase differences amount to about 3° in $^1S_0$, to about 1° in ^3P_I and to less than 0.2° in the higher partial waves. We are in the process of improving our procedure for extending two-nucleon potentials allowing Δ-isobar excitation.

IV. SUMMARY

The paper develops a novel momentum-space technique for solving the AGS equations without Coulomb for elastic nucleon-deuteron scattering and for nucleon-deuteron break-up. The technique is based on the expansion of the two-baryon transition matrix and of the deuteron wave function in terms of Chebyshev polynomials. The Chebyshev expansion is systematic and found to be highly efficient when used for interpolation. The solution of the AGS equations is carried out without any further approximation. The results agree very well with those obtained with alternative interpolation techniques.

The dynamics of three-nucleon scattering is based on the CD-Bonn potential; its charge dependence is kept in full for the $^1S_0$ partial wave and approximately for other isospin-triplet partial waves. Furthermore, that purely nucleonic reference potential is extended to include single Δ-isobar excitation; the standard technique for extension with exact phase equivalence at zero kinetic energy only is used. Δ-isobar effects on observables usually are quite moderate at the considered scattering energies, decisive only in special kinematic situations.

Using the CD-Bonn potential, we confirm most physics results for Δ-isobar effects obtained previously with the Paris potential. Noteworthy are the following special physics results of this paper:

(1) The A_y puzzle of elastic nucleon-deuteron scattering at 10 MeV nucleon lab energy cannot be resolved by a Δ-isobar effect, even if the Δ-mediated three-nucleon force has a spin-orbit contribution; the considered spin-orbit contribution is of short range, since it arises from the exchange of the ρ meson.

(2) The charge dependence of the two-nucleon interaction is important for nucleon-deuteron breakup in particular kinematic configurations.

(3) The removal of the Sagara discrepancy in the diffraction minima of the elastic differential nucleon-deuteron cross sections by the three-nucleon force derived from the Δ isobar is confirmed; the same effect is found in the minima of the nucleon analyzing power.

(4) Compared to our previous results, based on the Paris potential and its extension to the inclusion of a Δ isobar, some observables of elastic nucleon-deuteron scattering and of break-up get substantially changed in predictions based on CD Bonn and its extension to the inclusion of a Δ isobar. These changes are due to the fact that CD Bonn is the more modern potential accounting for the now existing database of two-nucleon scattering much better than the outdated Paris potential does.

APPENDIX A: CALCULATION OF CHEBYSHEV COEFFICIENTS

In this appendix, we give some important properties of the Chebyshev expansion of functions. More details can be found in Ref. [10].

The Chebyshev polynomial of degree i is

$$T_i(x) = \cos(i \arccos x). \tag{A1}$$

The Chebyshev polynomials are orthogonal in the interval $[-1,1]$ over the weight $(1-x^2)^{-1/2}$, i.e.,

$$\int_{-1}^{1} \frac{T_i(x)T_k(x)}{\sqrt{1-x^2}}\,dx = \frac{\pi}{2}\delta_{ik}(1+\delta_{i0}). \tag{A2}$$

The Gauss-Chebyshev quadrature formula

$$\int_{-1}^{1} \frac{f(x)}{\sqrt{1-x^2}}\,dx \approx \sum_{k=1}^{N} w_k f(x_k), \tag{A3}$$

the abscissas $x_k = \cos[(\pi/N)(k-\frac{1}{2})]$ being all the N zeros of $T_N(x)$ and the weights being $w_k = \pi/N$, were exact, if the function $f(x)$ could be expressed as a linear combination of Chebyshev polynomials up to degree $2N-1$. Using Eqs. (A2) and (A3), it is easy to show that the Chebyshev expansion of any arbitrary function $f(x)$, defined in the interval $[-1,1]$ as

$$f(x) \approx \sum_{i=0}^{n_c-1} c_i T_i(x), \tag{A4a}$$

with the Chebyshev coefficients

$$c_i = \frac{2-\delta_{i0}}{N}\sum_{k=1}^{N} f(x_k)T_i(x_k), \tag{A4b}$$

is exact for all x equal to the N zeros of $T_N(x)$, provided $n_c = N$.

What is the advantage of the Chebyshev expansion (A4) for the interpolation of the function $f(x)$, in comparison with interpolation schemes based on other polynomial? Suppose N is so large that the expansion (A4a) with $n_c = N$ is probably a perfect representation of $f(x)$. That representation is not necessarily more accurate than other polynomial expansions of the same order N, exact on some other set of N points. However, the truncated Chebyshev expansion (A4a) with $n_c = N_<$, $N_<$ being considerably smaller than N, may still be sufficiently accurate, since in typical cases the coefficients c_i are rapidly decreasing. In fact, if $f(x)$ has no singularities in the interval $[-1,1]$, the convergence of the Chebyshev expansion (A4) is *geometric*, i.e., $|c_i| \sim \exp(-\gamma i)$ for sufficiently large i. Singularities of $f(x)$ in the complex plane can slow down that convergence, but they can never destroy it, as demonstrated in Ref. [10]. The difference between the Chebyshev expansions (A4) with $n_c = N$ and $n_c = N_<$ can be no larger than the sum of the absolute values of all neglected Chebyshev coefficients $\Sigma_{i=N_<}^{N-1}|c_i|$, since all $|T_i(x)| \leq 1$. In fact, the error is dominated by $c_{N_<}T_{N_<}(x)$, an

oscillatory function with $N_<$ equal extrema distributed smoothly over the interval $[-1,1]$. This smooth spreading out of the error is a very important property of the Chebyshev expansion (A4): The Chebyshev expansion is close to the representation by the so-called *minimax polynomial*, which among all polynomials of the same degree has the smallest maximum deviation from the true function $f(x)$. That minimax polynomial is very difficult to find; the Chebyshev expansion is an efficient substitute for it.

The Chebyshev expansion (A4) can be extended to arbitrary intervals of definition by an appropriate mapping of $[-1,1]$ and to functions of several variables. When mapping to infinite or semi-infinite intervals, the convergence may become *subgeometric*, i.e., $|c_i| \sim \exp(-\gamma i^r)$ with $0 < r < 1$ for sufficiently large i. However, the asymptotic rate of convergence will often be academic for practical applications anyhow: The expansion (A4) may already be sufficiently accurate for the desired accuracy of the problem even without reaching the asymptotic region.

Finally, we give the definition of the Chebyshev coefficients of the two-baryon transition matrix and of the deuteron wave function as used in the calculations of this paper, i.e.,

$$\delta_{\chi'\chi}\frac{\delta(q'-q)}{q^2}T_{\eta'\eta}^{i'i}(\chi q, Z)$$

$$= \sum_{k',k=1}^{N} \bar{t}_{L'}^{i'}(p_{k'})_\alpha\langle p_{k'}q'\nu'(I'j')|$$

$$\times T_\alpha(Z)|p_k q \nu(Ij)\rangle_\alpha \bar{t}_L^i(p_k), \tag{A5a}$$

$$d_L^i = \sum_{k=1}^{N} \bar{t}_L^i(p_k)\langle p_k(LS)I_0 M_I T_0 M_{T_0}B|v_\alpha|dI_0 M_I T_0 M_{T_0}\rangle. \tag{A5b}$$

Here, the relative pair momenta p_k and $p_{k'}$ correspond to all the N zeros of $T_N(x)$, i.e., $T_N(x_c(p_k)) = T_N(x_c(p_{k'})) = 0$. The functions $\bar{t}_L^i(p_k)$ are defined to be

$$\bar{t}_L^i(p_k) = \frac{2-\delta_{i0}}{N}\frac{(p_k^2+a_L^2)^{L/2}}{p_k^L}T_i(x_c(p_k)); \tag{A5c}$$

they are related to the $t_L^i(p)$ of Eq. (6) used in the Chebyshev expansions (5) and (10).

APPENDIX B: THREE-NUCLEON BOUND STATE

At the three-nucleon bound state pole the inhomogeneous integral equation (1a) becomes the homogeneous one for the Faddeev amplitude $|\psi_\alpha\rangle$ of the bound state $|B\rangle$ with binding energy E_B, i.e.,

$$|\psi_\alpha\rangle = G_0(E_B)T_\alpha(E_B)P|\psi_\alpha\rangle, \tag{B1a}$$

$$|B\rangle = \mathcal{N}(1+P)|\psi_\alpha\rangle, \tag{B1b}$$

$\mathcal{N}$ being the normalization factor of the bound state. We solve the homogeneous integral equation (B1a) using Lanc-

TABLE I. Hadronic properties of tritium. Results for modern potentials CD-Bonn, AV18, Nijmegen I and II are listed and compared to those of the Paris potential. The Δ-isobar effect on the binding energy E_B is split up as arising from the two-nucleon dispersion ΔE_2 and from the effective three-nucleon force ΔE_3. The probability $P_{\mathcal{L}}$ of the wave function components refers to total three-baryon orbital angular momentum, $P_{3/2}$ to the $\mathcal{T}=\frac{3}{2}$ wave function component arising from charge dependence, and P_Δ to the wave function components with Δ-isobar configurations. All energies are given in MeV, all probabilities are given in percent; always three digits are quoted, only for the very small quantity $P_{3/2}$ four are quoted; they appear converged. With respect to the Chebyshev expansion, the results with 16 Chebyshev polynomials are already fully converged within this accuracy.

	E_B	ΔE_2	ΔE_3	P_S	$P_{S'}$	P_P	P_D	$P_{3/2}$	P_Δ
CD-Bonn	−8.004			91.621	1.307	0.047	7.020	0.0046	
CD-Bonn+Δ	−8.259	0.661	−0.916	88.797	1.210	0.072	7.232	0.0043	2.685
AV18	−7.627			90.132	1.291	0.066	8.509	0.0024	
AV18+Δ	−8.052	0.630	−1.055	87.500	1.145	0.095	8.780	0.0022	2.477
Nijmegen I	−7.740			90.286	1.268	0.066	8.375	0.0047	
Nijmegen I+Δ	−8.162	0.629	−1.051	87.552	1.125	0.096	8.634	0.0044	2.589
Nijmegen II	−7.660			90.312	1.290	0.064	8.329	0.0038	
Nijmegen II+Δ	−8.084	0.648	−1.072	87.661	1.145	0.095	8.604	0.0036	2.491
Paris	−7.462			90.112	1.392	0.064	8.431		
Paris+Δ	−7.820	0.590	−0.948	87.630	1.252	0.088	8.648		2.383
Experiment	−8.482								

zos method [25]. The dependence of the Faddeev amplitude on the pair momentum p is represented by Chebyshev polynomials in the form

$$G_0^{-1}(E_B)|\psi_\alpha\rangle \approx \sum_\nu \int q^2 dq \sum_{i=0}^{n_c-1} |t^i q \nu\rangle_\alpha (iq\nu|\psi_\alpha).$$
(B2)

The homogeneous integral equation (B1a) yields directly the Chebyshev coefficients $(iq\nu|\psi_\alpha)$, i.e.,

$$(i'q'\nu'|\psi_\alpha)$$

$$= \sum_{i''\nu''} \sum_{i\nu} \int_0^\infty q^2 dq \int_{-1}^1 dx \, \delta_{\chi'\chi''} T^{i'i''}_{\eta'\eta''}(\chi'q',E_B)$$

$$\times \frac{t^{i''}_{L''}(\bar{p}'(q',q,x))}{\bar{p}'^{L''}(q',q,x)} \frac{G_{\nu''\nu}(q',q,x)}{E_B - \delta\mathcal{M} - \frac{q'^2}{2\mu_\alpha} - \frac{q^2}{2\mu''_\alpha} - \frac{q'q}{m_\alpha}x}$$

$$\times \frac{t^i_L(\bar{p}(q',q,x))}{\bar{p}^L(q',q,x)}(iq\nu|\psi_\alpha).$$
(B3)

Resulting hadronic properties of the tritium bound state, i.e., the binding energy E_B and the wave function probabilities $P_{\mathcal{L}}$, P_Δ, and $P_{3/2}$, are shown in the Table I. We include partial waves up to total pair angular momentum $I=6$ in contrast to $I \leq 5$ used in remaining calculations of this paper; charge dependence and Δ-isobar coupling is treated as discussed for scattering. The contribution of the proton and neutron mass difference is evaluated perturbatively; it amounts 6–7 keV more binding for all potentials; that perturbative shift of energy is included in the quoted values for E_B. The inclusion of $I=6$ partial waves changes the tritium results by less than 2 keV for the binding energy E_B and by 0.001% for the wave function probabilities. Such a high accuracy is not needed for the existing nucleon-deuteron scattering data; there, we restrict the interaction to act in partial waves up to $I=5$. Our tritium results derived from purely nucleonic potentials agree with those of Ref. [26] within 1 keV for the binding energy E_B and within the accuracy given in Ref. [26] for the wave function probabilities.

APPENDIX C: SPLINE INTERPOLATION

The spline interpolation has the general form

$$f(x) \approx \sum_i f(x_i)S_i(x),$$
(C1)

with exact function values $f(x_i)$ at an appropriately chosen set of grid points and known functions $S_i(x)$ described in detail in Ref. [27]; we used a slightly different spline interpolation algorithm in Ref. [4], more appropriate there. Since the spline interpolation (C1) and the interpolation in terms of the Chebyshev polynomials (A4) have the same general structure, it is obvious that the numerical technique of this paper for solving integral equations (14) and (B3) can also be based on spline interpolation. The only difference is that the functions $t^i_L(p)$ and $\bar{t}^i_L(p_k)$, entering the definition of all arising matrix elements, are

$$t^i_L(p) = \frac{p^L}{(p^2+a_L^2)^{L/2}}S_i(p),$$
(C2a)

$$\bar{t}^i_L(p_k) = \frac{(p_k^2+a_L^2)^{L/2}}{p_k^L}\delta_{ik},$$
(C2b)

in case of spline interpolation. Of course, the grid points p_k are in this case not necessarily chosen as the zeros of a Chebyshev polynomial.

[1] S. Nemoto, K. Chmielewski, J. Haidenbauer, S. Oryu, P.U. Sauer, and N.W. Schellingerhout, Few-Body Syst. **24**, 213 (1998).

[2] S. Nemoto, K. Chmielewski, J. Haidenbauer, U. Meyer, S. Oryu, and P.U. Sauer, Few-Body Syst. **24**, 241 (1998).

[3] S. Nemoto, K. Chmielewski, S. Oryu, and P.U. Sauer, Phys. Rev. C **58**, 2599 (1998).

[4] K. Chmielewski, A. Deltuva, A.C. Fonseca, S. Nemoto, and P.U. Sauer, Phys. Rev. C **67**, 014002 (2003).

[5] L.P. Yuan, K. Chmielewski, M. Oelsner, P.U. Sauer, A.C. Fonseca, and J. Adam, Jr., Few-Body Syst. **32**, 83 (2002).

[6] L.P. Yuan, K. Chmielewski, M. Oelsner, P.U. Sauer, and J. Adam, Jr., Phys. Rev. C **66**, 054004 (2002).

[7] R. Machleidt, Phys. Rev. C **63**, 024001 (2001).

[8] E.O. Alt, P. Grassberger, and W. Sandhas, Nucl. Phys. **B2**, 167 (1967).

[9] C. Hajduk, P.U. Sauer, and W. Strueve, Nucl. Phys. **A405**, 581 (1983).

[10] J. P. Boyd, *Chebyshev and Fourier Spectral Methods* (Springer, Berlin, 1989).

[11] W. Glöckle, H. Witał̵a, D. Hüber, H. Kamada, and J. Golak, Phys. Rep. **274**, 107 (1996).

[12] M. Lacombe, B. Loiseau, J.M. Richard, R. Vinh Mau, J. Coté, P. Pirès, and R. de Tourreil, Phys. Rev. C **21**, 861 (1980).

[13] M. Allet *et al.*, Phys. Rev. C **50**, 602 (1994).

[14] C.R. Howell *et al.*, Few-Body Syst. **2**, 19 (1987).

[15] P.U. Sauer, K. Chmielewski, S. Nemoto, and S. Oryu, Nucl. Phys. **A684**, 531c (2001).

[16] R.B. Wiringa, V.G.J. Stoks, and R. Schiavilla, Phys. Rev. C **51**, 38 (1995).

[17] V.G.J. Stoks, R.A.M. Klomp, C.P.F. Terheggen, and J.J. de Swart, Phys. Rev. C **49**, 2950 (1994).

[18] A. Kievsky, Phys. Rev. C **60**, 034001 (1999).

[19] J. Strate *et al.*, Nucl. Phys. **A501**, 51 (1989).

[20] G. Rauprich, S. Lemaitre, P. Niessen, K.R. Nyga, R. Reckenfelderbäumer, L. Sydow, H. Paetz gen. Schieck, H. Witał̵a, and W. Glöckle, Nucl. Phys. **A535**, 313 (1991).

[21] M. Allet *et al.*, Few-Body Syst. **20**, 27 (1996).

[22] K. Sekiguchi *et al.*, Phys. Rev. C **65**, 034003 (2002).

[23] H. Shimizu, K. Imai, N. Tamura, K. Nisimura, K. Hatanaka, T. Saito, Y. Koike, and Y. Taniguchi, Nucl. Phys. **A382**, 242 (1982).

[24] K. Ermisch *et al.*, Phys. Rev. Lett. **86**, 5862 (2001).

[25] G. H. Golub and C. F. Van Loan, *Matrix Computations*, 3rd ed. (John Hopkins University Press, Baltimore, 1996).

[26] A. Nogga, Ph.D. thesis, Ruhr-Universität Bochum, 2001.

[27] W. Glöckle, G. Hasberg, and A.R. Neghabian, Z. Phys. A **305**, 217 (1982).